_____

PARTITIONING OF VOLATILE HALOCARBONS BETWEEN SURROGATES FOR ATMOSPHERIC SOLID AEROSOLS AND GAS PHASE AS EXAMINED BY TPD MS AND INVERSE GAS CHROMATOGRAPHY

V.I. Bogillo[1]*, M.S. Bazylevska[1], B.G. Mischanchuk[2], V.A. Pokrovskiy[2]

[1]*Department of Antarctic Geology and Geoecology*
Institute of Geological Sciences of National Academy of Sciences of Ukraine
55B Oles' Gonchar Street, Kyiv 01054, Ukraine
[2]*Chuiko Institute of Surface Chemistry of National Academy of Sciences of Ukraine*
17 General Naumov Street, Kyiv 03164, Ukraine

The desorption non-isothermal kinetics of preliminary adsorbed Cl, Br, and I-containing volatile halocarbons from the surface of surrogates for atmospheric solid aerosols (fumed silica and alumina, silica gel and H-mordenite) was studied by TPD MS. The TPD spectra demonstrate high heterogeneity of the surface studied. The average desorption activation energies and half-widths of the halocarbons desorption energy rectangular distribution were calculated. The relationships between the average desorption activation energies and molecular descriptors for the halocarbons were derived for the solids. The partitioning of the halocarbons and additional volatile organics between surrogates for mineral and carbonaceous atmospheric aerosols (silica gel, Carbopack S, Carbosil) was examined by using the inverse gas chromatography method. These data indicate to the energetic heterogeneity of the solid surfaces. The average adsorption energies and variances of the adsorption energy rectangular distribution were calculated and connected with molecular descriptors of the volatiles. A relationship is observed between average desorption activation energies of halocarbons on the silica gel surface from TPD MS data and average adsorption energies in these systems determined using inverse gas chromatography method at finite concentrations.

INTRODUCTION

The volatile F, Cl, Br and I-containing halocarbons (HCs) used as solvents and refrigerants are important priority toxic pollutants because exposure to the dangerous HCs can be injurious to human health and ecosystems [1]. Many of these compounds are toxic and exhibit mutagenic and/or carcinogenic properties. Major potential health effects of HCs exposure include acute and chronic respiratory effects, neurological toxicity, lung cancer, and eye and throat irritation.

The HCs participate in much heterogeneous industrial and natural processes. So, heterogeneous reactions of the HCs on the surface of stratospheric cryoaerosols are responsible for the development of the Antarctic ozone hole [2]. Release of chlorine during the HCs reactions with constituents of rocket exhaust formed by solid rocket motors (α- and γ-Al$_2$O$_3$) may provide an additional source of active chlorine that may catalytically destroy the stratospheric ozone [3].

Assessment of the importance of heterogeneous chemical reactions of HCs taking place on the surface of particulates present in the troposphere is an area of ongoing studies [4]. Heterogeneous transformations of HCs may decrease tropospheric oxidation potential which has been previously estimated from consideration of only gas-phase reactions of HCs with OH, NO$_3$ radicals and ozone [5, 6]. In case of such Langmuir-Hinshelwood heterogeneous reactions, the reaction coefficient depends on the adsorption energy of the HCs [7].

Potential of soils, sediments, ocean, snow and vegetation as sources and sinks for HCs has widely been discussed [8–11]. The volatile species can be transported over long distances from emission sources and be distributed between air and these environmental compartments. Adsorption of the HCs on these surfaces is a first stage of their removal from atmosphere and it determines the effectiveness of subsequent transformations such as photochemical, chemical and microbial oxidation, etc. Knowledge of HCs adsorption

* Corresponding author *vbog@carrier.kiev.ua*

characteristics from gas phase to such interfaces as water, snow, plants, rocks, soils, and sediments, organic, carbonaceous and mineral aerosols is important for assessing the partitioning and transport of the organics in our environment. The air/interface partition coefficients are involved as input parameters in current stationary and dynamic models of atmospheric and environmental chemistry [12]. However, these data for most atmospherically abundant HCs on various environmental interfaces are unknown.

Adsorption process is perhaps the most common method for the capture and recovery of HCs vapors, such as cleaning solvent vapors, from gas stream [13]. Most adsorbents play a role of catalyst in heterogeneous transformations of HCs or catalyst supports [14, 15]. Adsorption data for HCs are essential in choice and development of appropriate and selective adsorbents, solid sensors and in comprehension and the modeling of reaction kinetics on solid catalysts. In all cases, a priori prediction of the adsorption characteristics would be very useful in order to reduce the experimental efforts.

Inverse gas chromatography (IGC) [16] and thermal programmed desorption mass spectrometry (TPD MS) [17] would be appropriate methods for quantitative study of the HCs partitioning between gas phase and the solid surfaces. In the present work, we experimentally studied the partitioning of some Cl-, Br-, and I-containing volatile HCs between surrogates of mineral and carbonaceous aerosols and gas phase by using these methods.

EXPERIMENTAL

Materials. Following HPLC grade HCs (Merck, Germany) were used in the IGC and TPD MS study: dichloromethane (CH_2Cl_2), chloroform ($CHCl_3$), carbon tetrachloride (CCl_4), 1,2-dichloroethane ($C_2H_4Cl_2$), trichloroethylene (C_2HCl_3), dibromomethane (CH_2Br_2), bromoform ($CHBr_3$), 1,2-dibromoethane ($C_2H_4Br_2$), 1-bromobutane (C_4H_9Br), and methyl iodide (CH_3I). These HCs are emitted from industrial and natural sources [1]. Most of them are present in the troposphere in appreciable concentrations and, therefore, they affect the atmospheric level of HO_x (HO, HO_2) radicals and ozone. Furthermore, following volatile "test" compounds (Merck, Germany) possessing different electronic polarizability and acid-base characteristics of the molecules were used in the IGC study: *n*-pentane, *n*-hexane, *n*-heptane, benzene, carbon disulfide, acetonitrile, nitro-methane, nitroethane, methanol, ethanol, acetone, diethyl ether, tetrahydrofurane, and 1,4-dioxane.

The parameters of the Antoine equation and the liquid densities at the standard temperature (293 K) required to calculate their adsorption isotherms from IGC data are taken from [18].

Since the main component of terrigenous aerosols in the troposphere is silica [19] the silica gel S60 (Fluka, Switzerland) with BET specific adsorption surface area of $S_A = 336$ m²/g (as determined from low-temperature nitrogen adsorption measurements (77 K) by using an ASAP 2010 volumetric adsorption apparatus from Micromeritics (Norcross, GA)) and fumed silica Aerosil 300 (Chlorovinyl Co, Kalush, Ukraine) with $S_A = 267$ m²/g are chosen as this component. Second main component of the mineral aerosols is alumina [19] and the fumed alumina (Chlorovinyl Co, Kalush, Ukraine) with $S_A = 159$ m²/g was used in the TPD MS study. Zeolites are widely used as catalysts for dehalogenation processes of the HCs [15] and similar reactions are possible in the tropospheric conditions on the surface of mineral aerosols containing these minerals. A sample of commercial hydrogen mordenite (H-mordenite from Norton Co., USA) with $S_A = 380$ m²/g and with Si/Al = 10.7 was used in the TPD MS study.

Carbonaceous aerosols were imitated by graphitized carbon black (Carbopack C; Supelco, Bellefonte, PA, USA) with $S_A = 10$ m²/g and the silica gel modified by low-temperature carbonization of acetylacetone (Carbosil with 35 wt% carbon) with $S_A = 100$ m²/g [20]. The latter was chosen because the burning of solid fuels yields large amount of silica [19].

TPD-MS procedure. TPD MS technique has been developed, aimed at studies of adsorption-desorption kinetics and chemical transformations of HCs on the environmental surfaces starting from very low temperature (100 K). The equipment set included monopole mass analyzer MX-7304A (Ukraine, Sumy), liquid nitrogen free vacuum system and pump NMD 0.16–1, precise thermal regulator with heating element RIF-101, quarts-molybdenum tube for samples and IBM computer-guided system of registration and monitoring. Equipment parameters obtained in our test experiments are: mass range is 1–400 Dalton, resolving power is 10% intensity of 1/M, sensitivity is 10^{-8} g; the heating rate ranges from 0.05 to 30 K/min and average experiment duration is 1 hour. The adsorption capacity of the dispersed

solids has been provided desorption of about 10^{-3} times the weight of sample. The result is a gain in sensitivity of about 10^5 in comparison with bulk samples. All the experimental scheme of TPD of ultra-fine samples became similar to thermal analysis experiment with mass spectrometric detection of volatile products.

The dispersed samples of the solids each of about 0.1–1 mg weight are placed into a quartz-molybdenum tube and evacuated at 10^{-1} Pa and then attached to the inlet system of the mass spectrometer. The reactor-to-mass spectrometer interface included a high-vacuum valve with an orifice of diameter 5 mm and the inlet tube of 20 cm length which was kept at 150°C. The reaction space is open in the ion-source direction and at the heating rate used (about 0.1 K s^{-1}) the observed intensity of the ion current is expected to be proportional to the desorption rate so that diffusion retardation may be neglected. We assumed quasi-stationary conditions when the shape and position of desorption peaks did not depend on the temperature of the spectrometer interface, the sample dispersity and/or its size. The TPD data were not considered further if these conditions were not fulfilled.

In the typical TPD MS experiment the solid sample was preliminarily pressed at $3 \cdot 10^3$ Pa. This procedure, as it has been shown previously, does not change specific surface area of the fumed materials. Preliminary vacuum treatment of the samples was provided at the temperature 970 K during 2 hours. Sample pellet of size 2×2×1 mm has been introduced into quartz-molybdenum tube and evacuated at $7.5 \cdot 10^{-7}$ Pa for half of an hour. After cooling the sample down to room temperature the material has been exposed to a HC vapor in amount of inner volume of quartz-molybdenum tube i.e. about 10 cm^3. Then the sample was cooled down to the temperature of liquid nitrogen. Cooling lasted approximately 10 minutes. When the stationary temperature of the sample has been achieved, the high-vacuum pumping started and after five-minutes of pumping the cyclic record of mass spectra was switched on. The temperature has been recorded for each cycle and, correspondingly, to each mass spectrum. At the first stage of record the typical mass spectrum of a HC was observed, further all a HC was pumped away and only chemical background was observed in the mass spectrum. For example, characteristic temperature of 1,2-dichloroethane disappearance from the Aerosil 300 surface was 246°K.

IGC procedure. The inverse chromatographic measurements were carried out with gas chromatograph "LKhM 80" (Russia). Thermal conductivity detector was used in the study. The analog output from the detector was digitalized and recorded on an IBM PC computer controlled by original software (Turbo Pascal) to determine the coordinates of chromatographic peak from those measurements. Helium was used as the carrier gas. Air, as a non-interacting marker, was employed to measure the dead volume of the chromatographic column. Injection of the volatile compounds was repeated at least three times. Flow rate was measured at the end of the column with a bubble flow meter and its value was maintained in the range 30–40 cm^3/min. Pressures measured at the inlet and outlet of the column (scaling factor was 0.15 Pa) were applied to calculate the net retention volume. The molecular probes were injected manually with Hamilton glass micro syringes (Hamilton micro liter 700 and 7000 series syringe). The volume of injected liquid probes varied from 0.1 to 5 μl.

Short stainless columns (400 mm long and 3 mm I.D.) were filled by the examined solids. The columns were preliminary conditioned under helium at 470 K for 12 h before their use to remove the physically adsorbed water and other volatile traces from the solid surface. Adsorption measurements were carried out over a temperature range of from 353 to 453 K (at the isothermal conditions, scaling factor was 0.2 K) at 10 K interval. The temperatures of the detector and injector were 473 K.

Calculation of primary IGC data. The specific adsorption retention volume, V_S^o (in cm^3/m^2) for the examined molecular probes was calculated as

$$V_g^o = (t_X - t_0) \times \frac{F}{S_A w} \times \frac{273.15}{T_r} \times \frac{3}{2} \frac{\left(\frac{P_i}{P_0}\right)^2 - 1}{\left(\frac{P_i}{P_o}\right)^3 - 1} \times \frac{P_0 - P_{H_2O}}{P_0} \quad (1)$$

where t_X and t_0 are the retention times of the molecular probe and of the non-interacting marker (air) at column temperature T (in K), F is the flow rate of the carrier gas through column measured on the output at room temperature T_r, w is the weight of a solid in the column, P_{H_2O} is the saturated water vapor pressure at the T_r, P_i and P_O are the pressures of the carrier gas measured at the inlet and outlet of the column.

The "multiple injection" and "one-peak" methods are commonly applied to the analysis of

the chromatographic peak dependence on the known amount of the liquid probe injected into the chromatographic column, and for the subsequent determination of the adsorption isotherm on the surface of chromatographic support [21]. In both methods a given amount of probe injected quickly, inducing a peak. Adsorption or desorption may be followed by a mathematical examination of the front and tail of the recorded peak. The first method analyses the dependence of specific adsorption retention volume on the probe amount, whereas second approach deals with co-ordinates of the chromatographic peak at moderate or large amount of the probe.

The calculation of the vapor pressure for the molecular probes, P_{corr} and the surface solid coverage, a_{corr} for the adsorption isotherms using "one-peak" method with correction for multilayer adsorption [22] was carried out from the data for the peak' profile (400–2000 points) as follows

$$P = \left[\frac{R \times v_p \times \rho \times T}{MW \times S_{peak} \times F_{corr}} \right] \times h_i, \quad (2)$$

$$a = \left[\frac{v_p \times \rho}{MW \times S_{peak} \times S_A \times w} \right] \times S_{i(ads)}, \quad (3)$$

$$F_{corr} = \frac{3}{2} \frac{F \times T \times \left(1 - \frac{P_{H2O}}{P_o}\right)}{T_k} \times \frac{\left(\frac{P_i}{P_o}\right)^2 - 1}{\left(\frac{P_i}{P_o}\right)^3 - 1}, \quad (4)$$

$$P_{corr} = \frac{P}{1 - P/P_S}, \quad (5)$$

$$a_{corr} = \frac{a}{1 - P/P_S} \quad (6)$$

where R is the universal gas constant, v_p is the volume of the liquid probe injected, ρ is the liquid density at T_k, MW is the molecular weight, S_{peak} is the total area of the chromatographic peak calculated by its numerical integration, F_{corr} is the flow rate corrected by compressibility of the carrier gas in the column and change of surface tension for water in the bubble flow meter with the T_r value, h_i is the height for the point i localized on the descending side of the peak' tail, $S_{i(ads)}$ is the product of the distance on the chromatogram from the retention time of non-interacting marker to the retention time for point i on the height of the point, h_i, P_S is the saturated vapor pressure for the liquid probe at T.

RESULTS AND DISCUSSION

TPD MS measurements and calculation of desorption activation parameters. The desorption of the HCs preliminary adsorbed on the surrogates for mineral atmospheric particulates was studied by TPD MS method from liquid nitrogen up to room temperature. In all cases, observed mass spectra included reliably identified lines of HCs as a main component. The shape and temperature interval of evolution of molecular ion varied depending on the nature of the surrogate and adsorbed HCs. All mass spectra included also line of water of medium intensity, starting its evolution from the sample at the temperature of about 150 K for all samples.

Fig. 1 presents desorption peaks for the HCs from the silica gel surface. It is obvious that the shape of the peaks, their width and temperature maximum depend on the HCs structure.
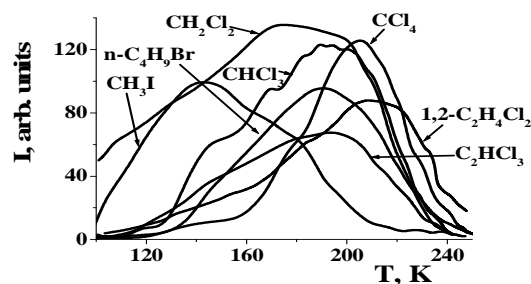

Fig. 1. TPD spectra of Cl, Br and I-containing volatile halocarbons preliminary adsorbed on the silica gel (Si60) surface. The heating rate was 0.1 K/s

For the interpretation of temperature dependencies of mass spectra we assume that the desorption equation may be expressed as a first-order process from homogeneous solid surface

$$d\Theta / dt = -k_D \Theta \quad (7)$$

where Θ is the surface coverage and the desorption rate coefficient, k_D is

$$k_D = A_D \exp(-E_D / RT) \quad (8)$$

where E_D is the desorption activation energy and A_D is the pre-exponential factor.

Both Eqs. (7) and (8) constitute the Polanyi-Wigner equation: $d\Theta / dt = -A_D \exp(-E_D / RT)$. At the initial condition $\Theta_{t=0} = 1$ we have the following solution of equation (7)

$$\Theta(t) = \exp[-\Phi(t)], \quad (9)$$

$$\Phi(t) = \int_0^t k_D dt. \quad (10)$$

According to Eq. (9) desorption rate which is proportional to ion current may be obtained in the following form

$$d\Theta(t)/dt = -k_D \exp[-\Phi(t)]. \qquad (11)$$

The key equation (10) may be expressed in an approximate analytical form for a slow heating rate ($\beta \leq 0.1$ K/s) and high values of the pre-exponential factor ($A_D > 10^9$ s^{-1}) assuming a linear heating rate, $T = T_0 + \beta t$ and expanding the temperature dependence near the peak' maximum T_{max}

$$\Phi(t) = \frac{RT_{max}^2}{E_D \beta} A_D \exp(-\frac{E_D}{RT}) \qquad (12)$$

which, in most cases, is valid within experimental accuracy. The condition of the maximum value of $d\Theta/dt$ (or ion current $I(t)$) is $\Phi(t) = 1$.

The behavior of $I(T)$ near the peak maximum may be used for calculating the parameters of non-isothermal kinetics. The behavior of the experimentally observed ion intensity $I(T)$ in the neighborhood of T_{max} may be written as

$$I(T)/I_{max} = 1 - \frac{I''\Delta T^2}{2} \qquad (13)$$

where $\Delta T = T - T_{max}$ and I'' is the value of the second derivative at the peak maximum of experimental curve $I = f(T)$.

Expanding, on the other hand, the expressions for ion current taking into account Eq. (12) and the condition $\Phi(t) = 1$ in the neighborhood of T_{max} and comparing with the chosen experimental values $\Delta T = T_{max} - T$ and corresponding $\Delta I = I_{max} - I$ one can easily obtain approximate formulas for the calculation of the desorption activation parameters

$$E_D = 8.27 T_{max} \sigma_D 10^{-3} \text{ [kJ/mol]} \qquad (14a)$$

and

$$A_D = \frac{\beta}{T_{max}} \sigma_D \exp(\sigma_D) \text{ [s}^{-1}\text{]}, \qquad (14b)$$

$$\sigma_D = 2\frac{T_{max}}{\Delta T}\sqrt{\frac{\Delta I}{I_{max}}} . \qquad (14c)$$

The determination of ΔT value and the corresponding $\Delta I / I_{max}$ from an experimental curve

depends upon two opposing factors. $\Delta T / T_{max}$ should be chosen as small as possible to preserve the validity of approximation made to derive equation (12); $\Delta I / I$, on the contrary, should be chosen as large as possible to decrease the error of graphical measurement of ΔI. A typical compromise is the value $\Delta I/I$ of about 0.1–0.3; the corresponding value of ΔT is found from the experimental peak $I = f(T)$. The values ΔI and ΔT should be derived from the low-temperature side of desorption peak. The existence of different adsorption sites on a solid surface being the most common source of the more or less overlapping peaks on the experimental TPD spectra. In case of first-order desorption from energetically heterogeneous surface it is necessary to introduce a normalized distribution function for surface sites over E_D values: $\rho(E_D)$. Then the total desorption rate $d\Theta/dt$ (and the total ion current, I) should be calculated as an integral

$$\frac{d\Theta}{dt}\int_0^\infty \frac{d\theta(t)}{dt}\rho(E_D)dE_D \qquad (15)$$

where $d\theta(t)/dt$ is the local desorption rate from the surface sites with desorption activation energy E_D at point t.

Unfortunately, very little information is available concerning $\rho(E_D)$ function in most cases of adsorption of organic molecules on the solid surfaces. In what follows condition $\Phi(t) = 1$ is applied to the simplest distribution function $\rho(E_D)$. Let function $\rho(E_D)$ be a rectangle in the interval $E_{D(min)}$, $E_{D(max)}$ of magnitude $(E_{D(max)} - E_{D(min)})^{-1}$. In this case

$$\frac{d\Theta}{dt} = \frac{1}{E_{D(max)} - E_{D(min)}} \int_{E_{D\,min}}^{E_{D(max)}} \frac{d\theta(E_D)}{dt}dE_D . \qquad (16)$$

Neglecting the weak pre-exponential dependencies upon T and E_D, and substituting E_D and T by average values T_{max} and $(E_{D(max)} + E_{D(min)})/2$, the following approximate expression may be obtained for this model

$$\frac{d\Theta}{dt} = \frac{\beta(E_{D(min)} + E_{D(max)})}{T_{max}(E_{D(max)} - E_{D(min)})} \times$$
$$\times \left[\Theta(E_{D(max)}, t) - \Theta(E_{D(min)}, t)\right] . \qquad (17)$$

Table 1. Average desorption activation energies ($E_{D(av)}$) and half-widths ($\Delta_D/2$) of the rectangular halocarbons desorption activation energy distributions of surfaces for surrogates of mineral aerosols from TPD MS data and evaporation enthalpies for the halocarbons, ΔH_{vap} from [18]

Halocarbon	A-300		Silica gel		Al$_2$O$_3$		H-mordenite		ΔH_{vap}
	$E_{D(av)}$	$\Delta_D/2$	$E_{D(av)}$	$\Delta_D/2$	$E_{D(av)}$	$\Delta_D/2$	$E_{D(av)}$	$\Delta_D/2$	
					kJ/mol				
CH$_2$Cl$_2$	50	20	70	10	64	10	67	17	28.0
CHCl$_3$	53	15	75	10	60	20	70	8	29.7
CCl$_4$	60	20	65	25	59	11	71	11	30.0
1,2C$_2$H$_4$Cl$_2$	54	20	70	10	67	15	75	15	32.0
C$_2$HCl$_3$	51	15	60	20	55	17	69	9	31.4
n-C$_4$H$_9$Br	55	13	75	15	73	17	78	16	33.0
CH$_3$I	42	12	60	10					27.2

Substitution of equations (9) and (12) in (17) gives the analytical dependence of the ion current upon the variables and parameters of the model

$$\frac{d\Theta}{dt} = \frac{\beta(E_{D(\min)} + E_{D(\max)})}{T_{\max}(E_{D(\max)} - E_{D(\min)})} \times$$

$$\times [\exp\left(-\frac{RT_{\max}^2}{\beta E_{D(\max)}} A_D e^{-\frac{E_{D(\max)}}{RT}}\right) - \quad (18)$$

$$-\exp\left(-\frac{RT_{\max}^2}{\beta E_{D(\min)}} A_D e^{-\frac{E_{D(\min)}}{RT}}\right)] \quad .$$

The observed great width of the desorption peaks (Fig. 1) points to the large energetic surface heterogeneity of the solids studied. The Eq. (11) is not reconcilable with experimental TPD spectra for all systems examined. Then the average desorption activation energies and half-widths of the rectangular desorption activation energy distributions were calculated assuming minimal pre-exponential desorption factor $A_D = 1.0 \cdot 10^{13}$ s^{-1} [23] with use of Eq. (18). These data are presented in Table 1.

From the Table we notice that both the average desorption activation energy and width of the distribution depend on the halocarbon structure and the solid surface. Maximum $E_{D(av)}$ values are obtained for H-mordenite and the minimum ones are characteristic of the Aerosil-300 surface.

One would expect the proximity of a $E_{D(min)}$ value for the physical desorption of preliminary adsorbed volatile compounds to the evaporation enthalpy of the compounds, ΔH_{vap}. However, as it is evident from the Table, the difference between a quantity $E_{D(av)} - \Delta_D/2$ and ΔH_{vap} varies from 2 to 30 kJ/mol. One of reason for this difference may be choice of very large pre-exponential factor A_D

for the evaporation process. Formerly we examined the non-isothermal desorption of water from silica surfaces by TPD MS and DTG methods [24] and for *n*-butanol desorption from silica gel surface by Q-TG and Q-DTG methods under quasi-equilibrium conditions [25]. The most calculations of A_D from the TPD spectra of water physically adsorbed on silica by using the most popular Polanyi-Wigner, Kissinger and Freeman methods [26] give lower desorption pre-exponential factors, ranging from 0.8 to $3.6 \cdot 10^5$ s^{-1}, than the vibrational frequency, 10^{13} s^{-1} [24]. The dramatic decrease of A_D was explained by limitations of the methods for independent evolution of A_D in the desorption kinetics from the heterogeneous solid surface [25]. An equation for estimation of the minimal A_D value in the TPD and Q-DTG studies of physically adsorbed liquids was proposed in [25]

$$A_{D(\min)} = \exp\left[\frac{\Delta H_{vap}}{RT_b} + \ln\left(\frac{\Delta H_{vap}}{RT_b}\right) - \ln\left(\frac{T_b}{\beta}\right)\right] \quad (19)$$

where T_b is the boiling temperature of the liquid at standard temperature, in K.

The calculation of the A_D values for HCs from Table 1 by Eq. (19) gives A_D varied from 90 s^{-1} (CCl$_4$) to 161 s^{-1} (*n*-C$_4$H$_9$Br). Because the approximate Redhead first-order desorption kinetic equation [25] predicts that difference between two desorption activation energies $E_{D(1)}$ and $E_{D(2)}$ is

$$E_{D(1)} - E_{D(2)} = RT_{\max}\left(\ln A_{D(1)} - \ln A_{D(2)}\right), \quad (20)$$

the decrease in A_D value from 10^{13} s^{-1} to 10^2 s^{-1} leads to the difference of ΔE_D up to 30 kJ/mol at $T_{max} \sim 150$ K. Then the $E_{D(av)}$ values from Table 1 would be shifted of about 30 kJ/mol in the low energy direction at $A_D \sim 10^2$ s^{-1}.

Almost all theoretical studies of TPD have been based on the absolute rate theory (ART) [27]. The inapplicability of the classical Polanyi-Wigner equation to describe the thermodesorption kinetics from real solid surfaces was known long ago. Various generalizations of the ART expressions, toward taking into account interactions between adsorbed molecules, energetic surface heterogeneity, existence of "precursor states" and other were proposed [27]. For example, Nagai showed [27] that the ART approach underestimates the role of entropy changes as an important factor affecting the kinetics of adsorption/desorption processes. The pre-exponential term for desorption rate includes product of molecular partition function of the adsorbed molecules, q_0^s and a constant characteristic for an adsorption system, ξ and they were treated as the best fit parameters in the Nagai theory whereas this term in the Kreuzer-Payne theory is: $A_D = S_0 \alpha_s kT (2\pi mkT / h) q_0^g / q_0^s$ where S_0 is a "sticking coefficient" on a "empty" surface, α_s is the "condensation" coefficient, q_0^g is the partition function of gas molecules related to the internal degrees of freedom. Also, the pre-exponential factor $K_D = (K_{gs} / q_0^s) \exp(-\mu_0^s / kT)$, where K_{gs} is a constant related to the exchange rate between gas phase and the solid surface once an isolated system has reached equilibrium, μ_0^s is the standard chemical potential of the adsorbed molecules, was proposed for the thermodesorption kinetics by using the Statistical Rate Theory of Interfacial Transport (SRTIT) [27]. The most parameters in above expressions are unknown or make sense as purely empiric. Then the A_D values are not limited by $T/2\pi h \sim 10^{13}$ s^{-1} as their downward boundary.

We attempt to describe the effect of HCs structure on the $E_{D(av)}$ values from Table 1 by using the quantitative "structure-activity" relationship (QSAR) similarly proposed in [28]

$$E_{D(av)} = a_1 \times \alpha_e + a_2 \times \Sigma\beta_2^H + a_3 \times \Sigma\alpha_2^H + a_4 \quad (21)$$

where α_e is the molecular deformation polarizability of a HC, $\Sigma\alpha_2^H$ and $\Sigma\beta_2^H$ are its acidity and basicity for the H-bond formation in the Abraham scale and coefficients a_1, a_2 and a_3 characterize average ability of surface solid sites to dispersive interaction, and the interaction with acid and base adsorbed molecules at H-bond formation while a_4 is a constant for given solid surface. The α_e, $\Sigma\alpha_2^H$ and $\Sigma\beta_2^H$ values for the HCs were taken from

[29, 30]. The calculated coefficients are presented in Table 2.

Table 2. Coefficients of Eq. (21) for thermodesorption of halocarbons from the surface of surrogates for atmospheric mineral aerosols

Coefficient	A-300	Silica gel	Al$_2$O$_3$	H-mordenite
a_1, kJ/(mol Å^3)	1.5±1.1	1.7±1.4		0.9±0.8
a_2, kJ/mol	54±42		113±43	51±25
a_3, kJ/mol	–	86±58	–	–
a_4, kJ/mol	41±13	45±16	60±15	61±9
R	0.756	0.668	0.897	0.916

As is evident from Table, the Eq. (21) adequately describes the desorption kinetics of HCs from the solids examined. The best result is obtained for H-mordenite whereas worst result is observed for silica gel (the lowest correlation coefficient R). High a_1 and a_2 coefficients denote the contributions of polarizability of surface sites and their acidity to desorption activation energy of HCs. As to H-mordenite, the terminal silanols (Si–OH), extra-framework AlOH groups and framework bridged Si–OH–Al species are its main Bronsted surface sites and their acidity in H-bond formation decreases as: SiOH > AlOH > Si–OH–Al [31]. This leads to the surface heterogeneity and to the high a_2 coefficient for the solid.

IGC measurements and calculation of the adsorption equilibrium parameters. The inverse chromatographic measurements were performed for 23 volatile organic compounds including 9 HCs on the surface of silica gel, Carbopack S and Carbosil. For all systems examined, we observed an appreciable dependence of the retention time on the probe amount. One example is displayed in Fig. 2. That the shapes of the tails of the peaks coincide for various amounts of the probe suggest that the observed asymmetry of the peaks has an equilibrium nature associated with nonlinearity of the adsorption isotherm rather than the diffusion kinetic one.

In all cases, adsorption isotherms calculated from the IGC data at various temperatures are concave with respect to the surface coverage axis (Fig. 3); i. e., they do not obey the Henry adsorption isotherm equation even at low coverage (below 10% of a monolayer). Although the Langmuir adsorption isotherm equation is more suitable to describe the isotherms in this coverage range, all the systems, except for *n*-alkanes/Carbopack exhibit significant deviations from the Langmuir equation.
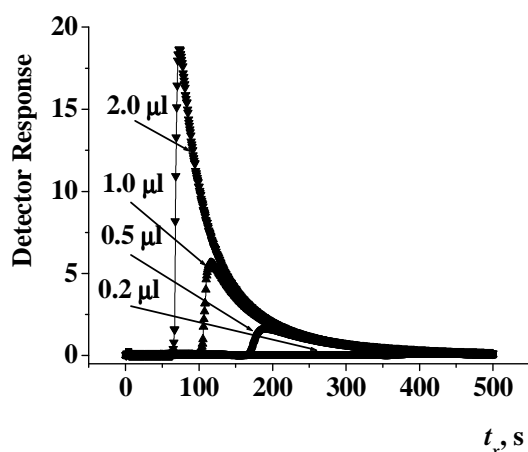
Fig. 2. Dependence of retention time and peak profile for CH_2Br_2/Carbosil system at 413 K on the amount of the liquid probe

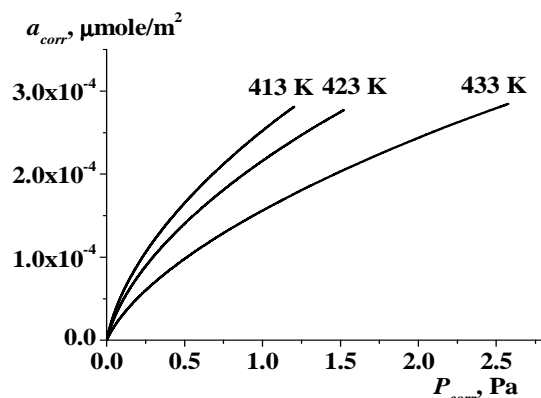**Fig. 3**. Adsorption isotherms at different temperatures for CH_2Br_2 on the Carbosil surface calculated from IGC data by using the "one peak" method
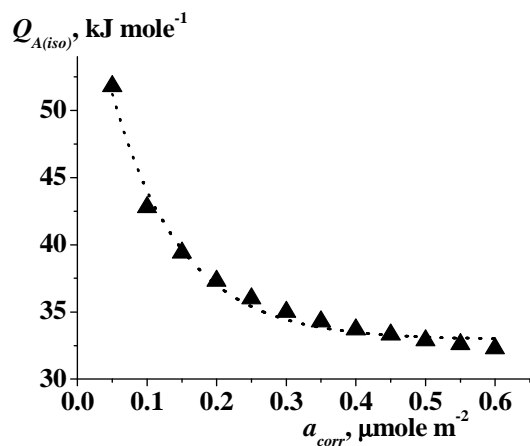

Fig. 4. Dependence of isosteric adsorption heat for CH_3I/Carbosil on the solid surface coverage

That the solid surfaces are heterogeneous is confirmed by the exponential fall of calculated isosteric adsorption heats as the surface coverage raises (Fig. 4). Therefore, the partitioning of the volatile organic compounds including HCs between the gas phase and the surface of the surrogates for solid atmospheric aerosols should be described with regard to the energetic heterogeneity of the surface similarly to above TPD MS data.

The common integral equation for the adsorption equilibrium from gas phase on the heterogeneous surface is [16]

$$\Theta(P,T) = \int_{E_{A(min)}}^{E_{A(max)}} \theta(P,T,E_A)\rho(E_A)dE_A \quad (22)$$

where $\Theta(P,T) = a_{corr}/a_m$ is the total relative surface coverage at P_{corr} and T, a_m is the monolayer capacity, $\theta(P,T,E_A)$ is the relative surface coverage of surface sites with adsorption energy E_A, $\rho(E_A)$ is the normalized differential adsorption energy distribution of the total surface, and $E_{A(min)}$ and $E_{A(max)}$ are the lower and upper boundaries of the distribution.

To solve Eq. (22), it is necessary to determine function $\theta(P,T,E_A)$. Let it be described by the Langmuir adsorption isotherm (lateral interaction between adsorbed molecules is ignored)

$$\theta(P,T,E_A) = \frac{\frac{P}{K_0}\exp\left(\frac{E_A}{RT}\right)}{1 + \frac{P}{K_0}\exp\left(\frac{E_A}{RT}\right)} \quad (23)$$

where K_0 is the Langmuir constant, which is given by [32]

$$K_0 = P_S \exp\left(\Delta H_{vap}/RT\right). \quad (24)$$

Eq. (22) can be readily solved by the improved regularization procedure [33]. Fig. 5*a-c* show the adsorption energy distributions of 3 halocarbons on the surfaces of Carbopack (*a*), Silica Gel (*b*) and Carbosil (*c*) calculated using this method. As can be seen, the narrowest unimodal distributions are observed for Carbopack, a solid with an energetically most homogeneous surface. For the Silica gel and Carbosil, several peaks in the distributions are observed. That several peaks appear is indicative of the existence of several types of adsorption sites with substantially different strengths on the solid surface.

The position and the shape of the distribution also depend on the halocarbon structure. In passing from CH_2Cl_2 to 1,2-$C_2H_4Cl_2$ and to *n*-C_4H_9Br, as the polarizability of the molecules increases, the peaks broaden and shift to higher adsorption energies.

a

b

c
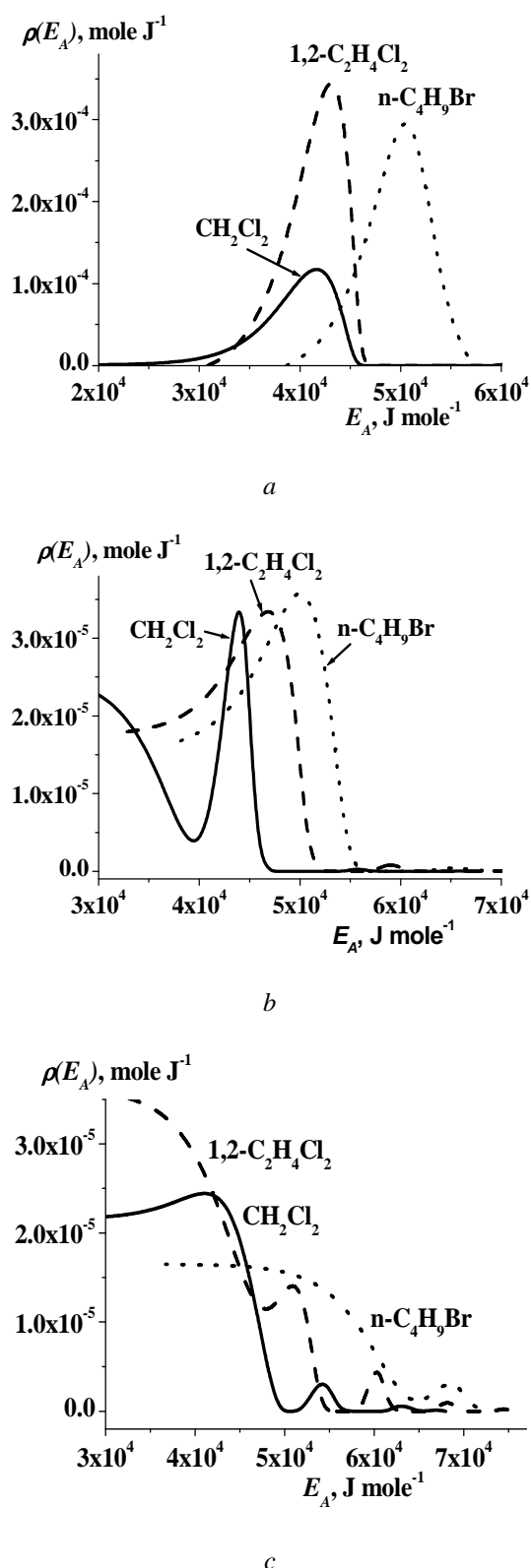
Fig. 5. Adsorption energy distributions for 3 halocarbons calculated by using the improved regularization procedure from IGC data *a* –on the Carbopack S surface; *b* – on the Silica Gel surface; *c* –on the Carbosil surface

Although the regularization procedure is effective in identifying the energetic heterogeneity of the solid surfaces, it is unsuitable for quantitative relationship between the molecular descriptors and the adsorption characteristics. Cumulants (semivariants) of the adsorption energy (or free adsorption energy) distributions, rather than the thermodynamic adsorption functions or the logarithms of the partition coefficient (which are used in the Henri law region), play the role of functions in the QSARs [34]. It is convenient to use in the QSARs the distribution functions that provide an analytical solution to Eq. (22). The simplest distribution that makes it possible to obtain an analytical solution is rectangular distribution

$$\rho(E_A) = \begin{cases} 1/(E_{A(max)} - E_{A(min)} \\ E_{A(min)} \leq E_A \leq E_{A(max)} \\ 0, E_A < E_{A(min)} ; E_A > E_{A(max)} \end{cases} \quad (25)$$

Using Eqs. (23) and (25), we obtain the solution to Eq. (22)

$$a_{corr} = \frac{a_m RT}{E_{A(max)} - E_{A(min)}} \times$$

$$\times \ln\left[\frac{1 + P_{corr} \exp(E_{A(max)}/RT - \ln K_0)}{1 + P_{corr} \exp(E_{A(min)}/RT - \ln K_0)}\right]. \quad (26)$$

The first- and second-order cumulants of the distribution (the average, K_I, and the variance, K_{II}) are given by

$$K_I = E_{A(av)} = (E_{A(max)} + E_{A(min)})/2, \quad (27)$$

$$K_{II} = \sigma_{Ea}^2 = \frac{E_{A(max)}^3 - E_{A(min)}^3}{3(E_{A(max)} - E_{A(min)})} - \quad (28)$$

$$-\frac{(E_{A(max)} + E_{A(min)})^2}{4}.$$

The calculated K_I, and K_{II} for the adsorption systems examined by IGC are presented in Table 3. They are related to molecular descriptors for halocarbons and other volatiles by Eq. (21). The table shows that, in passing from carbon black (which has an energetically nearly homogeneous surface) to Silica Gel and to Carbosil, the variances increase markedly. The results of regression analysis for Eq. (21) are given in Table 4.

As can be seen from these data, the mean polarizability of the solid surface sites increases as Carbopack>Carbosil>Silica Gel, the mean acidity in the H-bond formation as Silica Gel>Carbosil>Carbopack and the mean basicity in the H-bond formation as Carbosil≈Carbopack>Silica Gel. The last sequence is explained by existence of strong basic sites, such as basal faces of graphite, which can be considered as π-electron condensed systems, ~C=O and ~C(O)OH groups. The reason for decay of surface acidity from Silica Gel to Carbosil is the decrease in the hydroxyl groups concentration and their activity after carbonization of silica surface.

Table 3. Molecular descriptors of volatile organic compounds, their average adsorption energies ($E_{A(av)}$, in kJ mol^{-1}) and the adsorption energy variances (σ^2_{Ea}, in kJ^2 mol^{-2}) on the solid surfaces

| Compound	Molecular descriptors			Carbopack		Carbosil		Silica Gel	
	α_e, A^3	$\Sigma\alpha_2^H$	$\Sigma\beta_2^H$	$E_{A(av)}$	σ^2_{Ea}	$E_{A(av)}$	σ^2_{Ea}	$E_{A(av)}$	σ^2_{Ea}
CH_2Cl_2	6.48	0.10	0.05	28.0	104.2	33.0	143.6	28.8	136.8
$CHCl_3$	8.51	0.15	0.02	42.3	0.08	34.1	162.4	28.4	120.6
CCl_4	10.48	0	0	41.7	0.03	37.0	150.2	28.7	88.6
$1,2\text{-}C_2H_4Cl_2$	8.0	0.10	0.11	43.1	0.10	37.7	169.1	36.7	63.3
CH_2Br_2	9.32	0.10	0.10	36.0	1.60	34.0	156.9	29.5	124.2
$CHBr_3$	11.82	0.15	0.09	44.0	0.31	39.3	181.3	30.5	115.2
$1,2\text{-}C_2H_4Br_2$	11.26	0.10	0.17	46.7	0.14	40.9	165.9	33.3	129.2
C_4H_9Br	13.9	0	0.12	50.7	0.0045	46.0	168.4	35.5	151.8
CH_3I	7.97	0	0.13	25.4	104.7	31.9	123.5	25.9	119.6
$n\text{-}C_5H_{12}$	9.99	0	0	43.8	0.00008	33.5	127.8	23.4	130.1
$n\text{-}C_6H_{14}$	11.76	0	0	48.4	0.00017	38.2	176.5	29.8	65.6
$n\text{-}C_7H_{16}$	13.61	0	0	53.3	0.00002	41.3	158.2	32.8	105.1
C_6H_6	10.33	0	0.14	47.7	13.2	38.0	160.1	35.4	61.2
CH_3OH	3.29	0.43	0.47	32.0	103.6	45.6	156.4	41.8	140.2
C_2H_5OH	5.11	0.37	0.48	37.4	129.8	50.7	170.4	46.7	156.1
$(CH_3)_2C=O$	6.40	0.04	0.49	28.4	108.6	38.8	148.7	37.5	136.2
$(C_2H_5)_2O$	10.2	0	0.45	41.6	8.3	37.4	149.8	33.5	157.4
C_4H_8O	8.2	0	0.48	31.1	29.5	39.6	165.8	39.8	138.4
$C_4H_8O_2$	10.0	0	0.64	43.1	0.95	37.2	106.8	44.1	164.2
CH_3CN	4.40	0.07	0.33	25.1	107.2	40.2	155.8	34.6	141.9
CH_3NO_2	7.37	0.06	0.32	26.6	0.00001	37.1	151.8	37.5	67.8
$C_2H_5NO_2$	9.63	0.02	0.33	33.3	0.00001	41.6	173.6	38.0	121.3
CS_2	6.9	0	0.07	37.3	120.3	32.1	141.3	26.9	115.6

Table 4. Coefficients of Eq. 21 for partitioning the volatile organic compounds between gas phase and solid surface

Function/ Coefficient	Carbopack S	Silica Gel	Carbosil
	$E_{A(av)}$		
a_1, kJ/(mol A^3)	3.1±0.5	0.7±0.3	1.0±0.3
a_2, kJ/mol	–	25.3±3.6	11.6±3.8
a_3, kJ/mol	29.2±10.6	19.4±6.8	30.0±7.0
a_4, kJ/mol	9.8±5.4	21.1±3.4	24.4±3.6
R	0.85	0.88	0.77
	σ^2_{Ea}		
a_1, kJ^2/(mol^{2}A^6)	-15.7±3.5	–	2.8±1.7
a_2, kJ^2/mol^2	–	84.0±33.0	–
a_3, kJ^2/mol^2	–	–	89.0±37.0
a_4, kJ^2/mol^2	182.0±39.0	84.0±32.0	126.0±19.0
R	0.78	0.55	0.52

The proposed approach makes it possible to establish how the variance of the adsorption energy distribution depends on the molecular descriptors. The variance is determined by both the chemical heterogeneity of the surface sites and their topography. As can be seen, the largest contribution to the variance for Carbopack comes from the sites polarizability; for Carbosil the contribution from basic sites is also important. Acidic sites markedly influence the variance only for Silica Gel, which surface contains various types of silanol groups (single, vicinal and geminal).

Relationship between TPD MS and IGC data. As it shown from Fig. 6, a relationship is observed between average desorption activation energies of HCs on the silica gel surface from TPD MS data and average adsorption energies in these systems determined using IGC method at finite concentrations. More low $E_{A(av)}$ values in comparison with $E_{D(av)}$ are explained by more high temperatures in the IGC experiment (from 353 to 453 K) as against the TPD MS experiment

(from 100 to 298 K) and by difference between pre-exponential desorption factor used in the TPD kinetics and average adsorption entropy for the HCs in the IGC study.
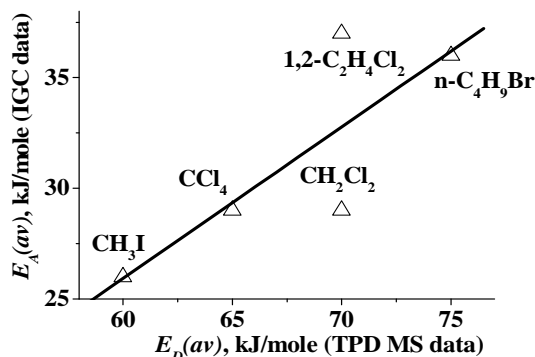
Fig. 6. Relationship between average desorption activation energies (TPD MS data) and average adsorption energies (IGC data) for halocarbons on silica gel surface

The calculated coefficients a_1, a_2 and a_3 of Eq. (21) from TPD MS and IGC data lie within the same order. Thus, the proposed approach makes it possible to estimate average desorption activation energy and adsorption energy for the HCs on the basis of their molecular descriptors.

Compensation effect in the partitioning of HCs on the heterogeneous solid surface. All above calculations of K_I and K_{II} values from IGC data were carried out in assumption that K_0 constant is independent on the surface coverage. In case of dependence of K_0 on the $\Theta(P,T)$ value, the integral adsorption equation should include in addition to $(\rho(E_A))$ function, the surface distribution on the $ln\ K_0$ value, $\rho(ln\ K_0)$ also

$$\Theta(P,T) = \iint_{\Delta E_A, \Delta \ln K_0} \theta(P,T,E_A,\ln K_0)\rho(E_A)\rho(\ln K_0)dE_A d\ln K_0 \cdot (29)$$

Two extreme variants for behavior of the K_0 and E_A values can be proposed: there are correlation between these parameters and its lack. Because $K_0 = \exp(-\Delta S_A / R)$ where ΔS_A is the molar isosteric adsorption entropy, the decrease of molar isosteric adsorption enthalpy may lead to fall of the adsorption entropy. Such relationship between enthalpy and entropy in phase transitions and intermolecular complex formation is well known as "compensation effect" or "isoequilibrium relationship" [35]. In first time the adsorbing molecules interact with most active sites of the heterogeneous surface at low vapor pressure

(high E_A values). Then the P value increases and less active sites are filled up. This results in decrease of $-\Delta S_A$ function and the K_0 constant. The "isoequilibrium relationship" between E_A and K_0 may be written as

$$\ln K_0 = \ln K_{0(iso)} + E_A / RT_{iso} \qquad (30)$$

where $K_{0(iso)}$ is the K_0 value at isoequilibrium temperature T_{iso}, when the Langmuir constant are equal for all surface sites, i. e. the surface is homogeneous over these constants.

It has been shown that logarithm of the Langmuir constant for HCs decreases with reducing the adsorption energy as the surface coverage of Silica Gel increases and compensation effect has been observed [36]. Such relationship between E_A and $ln\ K_0$ is displayed in Fig. 7 for CH_3I/Carbosil system.
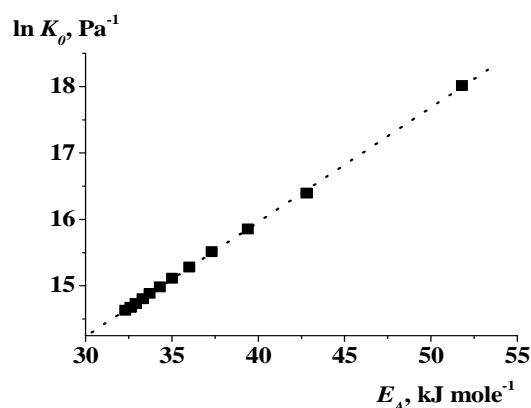
Fig. 7. Variation of the Langmuir constant versus adsorption energy for the CH_3I/Carbosil system

The approaches based on the distribution moments theory and condensation approximation have been proposed to evaluate parameters of this dependence from the adsorption data and the calculation has been performed for the adsorption of chloromethanes series (CH_nCl_{4-n}, n = 0÷3) and methyl iodide on Silica Gel and Carbosil surface [36]. For example, $K_{0(iso)} = 8.7 \cdot 10^3$ Pa^{-1} and $T_{iso} = 700$ K were obtained for the CH_3I/Carbosil system. The range of the Langmuir constants at several coverages exceeds noticeably ones calculated by Eq. (24): $\ln K_{0(calc)} = 12.2 - 12.8$ Pa^{-1} for the chloromethanes series on Silica Gel and the experimental $\ln K_{0(exp)}$ values varied from 5.7 to 20.8 Pa^{-1} as the relative surface coverage falls from 1.0 to 0. These variations should be taken into account in the calculations of the $\rho(E_A)$ function from the adsorption data.

Atmospheric implications. As it follows from above TPD MS and IGC data, the surfaces of components of atmospheric mineral and carbonaceous aerosols are energetically heterogeneous. Only Langmurian adsorption equilibrium on the homogeneous surfaces (or its initial linear part of the isotherms, i. e. Henry region) is considered in current models of heterogeneous atmospheric chemistry [37]. The approximation of homogeneous surface may overestimate the partition coefficients and adsorption enthalpies, since these quantities usually calculated from adsorption measurements in the Henry region, i. e., under conditions where only the strongest adsorption sites are involved. The fraction of such active sites at the surface of atmospheric particles can be extremely small, and, therefore, these quantities are not suitable for describing the activity of their surface as a whole.

The surface of the atmospheric solid aerosols is chemically and structurally heterogeneous [7, 38], which can be explained by its containing many types of adsorption sites with various activities, by difference in the topography of such sites and by the specifics of the amorphous structure of the surface layer and porous structure of the particles. Therefore, the partitioning of HCs and other volatile impurities between the surface of aerosol particles and air is convenient to calculate within the framework of the above approaches developed for describing the adsorption of species from the gas phase on a heterogeneous solid surface. The proposed approach (Eqs. (21), (26)–(28)) makes possible to estimate the volatile structure, the temperature influence the partition coefficients and the surface concentrations on the aerosol particles.

REFERENCES

1. The Handbook of Environmental Chemistry / Ed. P. Fabian, O.N. Singh. – V. 4, Part E. Reactive Halogen Compounds in the Atmosphere – Heidelberg, Germany: Springer, 1999. – 221 p.

2. *Solomon S.* Stratospheric ozone depletion: a review of concept and history // Rev. Geophys. – 1999. – V. 37, N 3. – P. 275–316.

3. *Robinson G.N., Freedman A., Kolb C.E., Worsnop D.R.* Decomposition of halomethanes on α-alumina at stratospheric temperature // Geophys. Res. Lett. – 1994. – V. 21. – P. 377–380.

4. *Kutsuna S., Takeuchi K., Ibusuki T.* Laboratory study on heterogeneous degradation of methyl chloroform (CH_3CCl_3) on aluminosilica clay minerals as its potential tropospheric sink // J. Geophys. Res. – 2000. – V. 105. – P. 6611–6620.

5. *Zakharenko V.S., Parmon V.N.* Remediation of the Earth's atmosphere throgh photoinitiated destruction of freons on the alkaline earth oxide components of tropospheric aerosols // Colloid. Surf. A. – 1999. – V. 151. – P. 367–376.

6. *Isidorov V.A.* Organic chemistry of the Atmosphere. – St. Petersburg: Khimizdat, 2001. – 351 p.

7. *Bogillo V.I.* Impact of mineral aerosols composition on the kinetics of the heterogeneous fate of trace volatiles from atmosphere // Chem. Phys. Technol. Surf. – 2010. – V. 1. – N 1. – P. 36–47.

8. *Bogillo V.I., Bazylevska M.S., Borchers R.* Past and future for ozone-depleting halocarbons in Antarctic environment // Role of Interfaces in Environmental Protection NATO Sci. Ser. (IV. Earth Environ. Sci. V. 24) / Ed. S. Barany. – Dordrecht: Kluwer Acad. Publ., 2003. – P. 161–168.

9. *Bogillo V.I., Borchers R., Bazylevska M.S.* Formation and sinks of volatile trace compounds in coastal Antarctica // Terra Nostra. – 2004. – V. 4. – P. 109–110.

10. *Keppler F., Eiden R., Nirdan V. et al.* Halocarbons produced by natural oxidation processes during degradation of organic matter // Nature. – 2000. – V. 403. – P. 298–301.

11. *Carpenter L.J., Hopkins J.R., Jones C.E. et al.* Abiotic source of reactive organic halogens in the Sub-Arctic atmosphere? // Environ. Sci. Technol. – 2005. – V. 39, N 22. – P. 8812–8816.

12. *Stroebe M., Scheringer M., Held H., Hungerbühler K.* Inter-comparison of multimedia modelling approaches: modes of transport, measures of long range transport potential and the spatial remote state // Sci. Total Environ. – 2004. – V. 321. – P. 1–20.

13. *Kawasaki N., Tanada S., Nakamura T., Abe I.* The recovery of chlorofluorocarbons and chlorofluorocarbon replacements by surface modified activated carbon // J. Colloid. Interface Sci. – 1995. – V. 172. – P. 368–373.

14. *Kovalchuk V.I., d'Itri J.L.* Catalytic chemistry of chloro- and chlorofluorocarbon dehalogenation: from macroscopic observations to molecular level understanding // Appl. Catal. A. – 2004. – V. 271. – P. 13–25.

15. *Howe R.F.* Zeolite catalysts for dehalogenation processes // Appl. Catal. A. – 2004. – V. 271. – P. 3–11.

16. *Bogillo V.I., Shkilev V.P., Voelkel A.* Determination of surface free energy components for heterogeneous solids by means of inverse gas chromatography at finite concentrations // J. Mat. Chem. – 1998. – V. 8, N 9. – P. 1953–1961.

17. *Pokrovskiy V.A.* Temperature-programmed desorption mass spectrometry (TPD MS) of dispersed oxides // Adsorpt. Sci. Technol. – 1997. – V. 14, N 5. – P. 301–317.

18. *Reid R., Prausnitz J.M., Sherwood T.* The Properties of Gases and Liquids / 3rd ed. – New Tork: McGraw-Hill, 1977. – 576 p.

19. *Pokrovskiy V.A., Bogillo V.I., Dabrowski A.* Adsorption and chemisorption of organic pollutants on the solid aerosols surface // Adsorption and its Application in Industry and Environmental Protection / Ed. A. Dabrowski. – Amsterdam: Elsevier, 1999. – P. 571–634.

20. *Turov V.V., Leboda R., Bogillo V.I., Skubishewska-Zieba J.* Adsorption of water on the surface of mesoporous silicas and carbosils as examined by 1H nuclear magnetic resonance spectroscopy // Langmuir. – 1997. – V. 13, N 5. – P. 1237–1244.

21. *Conder J.D., Young C.L.* Physicochemical Measurements by Gas Chromatography. – New York: Wiley, 1979. – 267 p.

22. *Balard H.* Estimation of the surface energetic heterogeneity of a solid by inverse gas chromatography // Langmuir. – 1997. – V. 13, N 5. – P. 1260–1269.

23. *Zhdanov V.P.* Elementary Physicochemical Processes on the Surface. – Novosibirsk: Nauka, 1988. – 319 p. (in Russian).

24. *Bogillo V.I., Pirnach L.S., Dabrowski A.* Monte Carlo simulation of silica surface dehydroxylation under nonisothermal conditions // Langmuir. – 1997. – V. 13, N 5. – P. 928–935.

25. *Bogillo V I., Staszczuk P.* Characterization of the structural and energetic heterogeneity of mesoporous solid surfaces from Q-DTG data // J. Therm. Anal. Calorim. – 1999. – V. 55, N 2. – P. 493–510.

26. *deJong A.M., Niemantsverdriet J.W.* Thermal desorption analysis: comparative test of ten commonly applied procedures // Surf. Sci. – 1990. – V. 233. – P. 355–365.

27. *Rudzinski W., Borowiecki T., Panczyk T., Dominko A.* On the applicability of Arrhenius plot methods to determine surface energetic heterogeneity of adsorbents and catalysts surfaces from experimental TPD spectra // Adv. Colloid Interfaces Sci. – 2000. – V. 84. – P. 1–26.

28. *Bazylevska M.S., Bogillo V.I.* Description of air/surface partitioning for volatile organic pollutants in Antarctic environment // Role of Interfaces in Environmental Protection NATO Sci. Ser. (IV. Earth Environ. Sci. V. 24) / Ed. S. Barany. – Dordrecht: Kluwer Acad. Publ., 2003. – P. 153–160.

29. CRC Handbook of Chemistry and Physics / 77th ed. – Boca Raton: CRC. – 1996. – 1539 p.

30. *Abraham M.H., Andonian-Haftvan J., Whiting G.S., Leo A.* Hydrogen bonding. Part 34. The factors that influence the solubility of gases and vapours in water at 298 K, and a new method for its determination // J. Chem. Soc. Perkin Trans. II. – 1994. – P. 1777–1791.

31. *Su B.-L., Norberg V.* Quantitative characterization of H-mordenite zeolite structure by infrared spectroscopy using benzene adsorption // Colloids Surf. – 2001. – V. 187–188. – P. 311–318.

32. *Jaroniec M., Madey R.* Physical Adsorption on Heterogeneous Solids. – Amsterdam: Elsevier, 1988. – 351 P.

33. *Bogillo V.I., Shkilev V.P.* Evaluation of desorption energy distributions from TPD spectra on a heterogeneous solid surface // J. Therm. Anal. Calorim. – 1999. – V. 55, N 2. – P. 483–492.

34. *Bogillo V.I.* Kinetics of organic compounds chemisorption from gas phase on oxide surfaces // Adsorption on New and Modified Inorganic Sorbents / Ed. A. Dabrowski, V.A. Tertykh. – Amsterdam: Elsevier, 1996. – P. 135–184.

35. *Liu L., Guo O.-X.* Isokinetic relationship, isoequilibrium relationship, and enthalpy-entropy compensation // Chem. Rev. – 2001. – V. 101. – P. 673–695.

36. *Bogillo V.I., Bazylevska M.S.* Compensation effect in adsorption on heterogeneous solid surface // Ukr. Khim. Zh. – 2006. – V. 72, N 8. – P. 78–84.

37. *Crowley J.N., Ammann M., Cox R.A. et al.* Evaluated kinetic and photochemical data for atmospheric chemistry: Volume V – Heterogeneous reactions on solid sub-strates // Atmos. Chem. Phys. Discuss. – 2010. – V. 10. – P. 5233–5564.

38. *Bogillo V.I.* The particle morphology effect of atmospheric aerosols on the interaction kinetics with volatile impurities // Chem. Phys. Technol. Surf. – 2010. – V. 1. N. 2. – P. 148–165. (in Russian).

Дослідження розподілу легколетких галогенвуглеводнів між сурогатами атмосферних твердих аерозолів і газовою фазою методами ТПД МС і оберненої газової хроматографії

В.Й. Богилло, М.С. Базилевська, Б.Г. Місчанчук, В.О. Покровський

Відділ геології та геоекології Антарктики, Інститут геологічних наук Національної академії наук України
вул. Олеся Гончара 55Б, Київ 01054, Україна, vbog@carrier.kiev.ua
Інститут хімії поверхні ім. О.О. Чуйка Національної академії наук України
вул. Генерала Наумова 17, Київ 03164, Україна

Кінетика неізотермичної десорбції попередньо адсорбованих Cl, Br і I-вмістних галогенвуглеводнів (ГВ) з поверхні сурогатів атмосферних твердих аерозолів (пірогенні кремнезем і оксид алюмінію, силікагель і Н-морденіт) вивчена методом температурно-програмованої десорбційної мас-спектрометрії (ТПД МС). ТПД спектри демонструють високу неоднорідність вивчених поверхонь. Розраховані середні величини енергії активації десорбції та півширини прямокутних розподілів енергій десорбції ГВ. Отримані співвідношення між середніми енергіями активації десорбції ГВ і їх молекулярними дескрипторами для всіх вивчених твердих тіл. Розподіл ГВ і додаткових летких органічних сполук між сурогатами мінеральних і вуглецьвмісних атмосферних аерозолів (силікагель, Карбопак і Карбосіл) досліджено методом оберненої газової хроматографії (ОГХ). Дані ОГХ вказують на енергетичну неоднорідність поверхні цих твердих тіл. Розраховані середні величини енергії адсорбції ГВ і дисперсії прямокутного розподілу поверхонь по енергіям адсорбції та знайдені зв'язки між цими величинами та молекулярними дескрипторами цих летких сполук. Встановлено співвідношення між середніми енергіями активації десорбції ГВ з силікагелю з даних ТПД МС і середніми енергіями адсорбції в цих системах, визначеними з даних ОГХ при скінченних концентраціях.

Исследование распределения легколетучих галогенуглеводородов между суррогатами атмосферных твердых аэрозолей и газовой фазой методами ТПД МС и обращенной газовой хроматографии

В.И. Богилло, М.С. Базилевская, Б.Г. Мисчанчук, В.А. Покровский

Отдел геологии и геоэкологии Антарктики, Институт геологических наук Национальной академии наук Украины
ул. Олеся Гончара 55Б, Киев 01054,Украина, vbog@carrier.kiev.ua
Институт химии поверхности им. А.А. Чуйко Национальной академии наук Украины
ул. Генерала Наумова 17, Киев 03164, Украина

Кинетика неизотермической десорбции предварительно адсорбированных Cl, Br и I-содержащих галогенуглеводородов (ГУ) с поверхности суррогатов атмосферных твердых аэрозолей (пирогенные кремнезем и окись алюминия, силикагель и Н-морденит) изучена методом температурно-программированной десорбционной масс-спектрометрии (ТПД МС). ТПД спектры демонстрируют высокую неоднородность изученных поверхностей. Рассчитаны средние значения энергии активации десорбции и полуширины прямоугольных распределений энергий десорбции ГУ. Получены соотношения между средними величинами энергии активации десорбции ГУ и их молекулярными дескрипторами для всех изученных твердых тел. Распределение ГУ и добавочных летучих органических соединений между суррогатами минеральных и углеродсодержащих атмосферных аэрозолей (силикагель, Карбопак и Карбосил) исследовано методом обращенной газовой хроматографии (ОГХ). Данные ОГХ указывают на энергетическую неоднородность поверхности этих твердых тел. Рассчитаны средние энергиии адсорбции ГУ и дисперсии прямоугольного распределения поверхностей по энергиям адсорбции и найдены связи между этими величинами и молекулярными дескрипторами летучих соединений. Установлено соотношение между средними энергиями активации десорбции ГУ с силикагеля из данных ТПД МС и средними энергиями адсорбции в этих системах, определенными из данных ОГХ при конечных концентрациях.